PDGF-BB Carried by Endothelial Cell–Derived Extracellular Vesicles Reduces Vascular Smooth Muscle Cell Apoptosis in Diabetes

Gabriele Togliatto,[1] Patrizia Dentelli,[1] Arturo Rosso,[1] Giusy Lombardo,[1] Maddalena Gili,[1] Sara Gallo,[1] Chiara Gai,[1] Anna Solini,[2] Giovanni Camussi,[1] and Maria Felice Brizzi[1]

Diabetes 2018;67:704–716 | https://doi.org/10.2337/db17-0371

Endothelial cell–derived extracellular vesicles (CD31EVs) constitute a new entity for therapeutic/prognostic purposes. The roles of CD31EVs as mediators of vascular smooth muscle cell (VSMC) dysfunction in type 2 diabetes (T2D) are investigated herein. We demonstrated that, unlike serum-derived extracellular vesicles in individuals without diabetes, those in individuals with diabetes (D CD31EVs) boosted apoptosis resistance of VSMCs cultured in hyperglycemic condition. Biochemical analysis revealed that this effect relies on changes in the balance between antiapoptotic and proapoptotic signals: increase of bcl-2 and decrease of bak/bax. D CD31EV cargo analysis demonstrated that D CD31EVs are enriched in membrane-bound platelet-derived growth factor-BB (mbPDGF-BB). Thus, we postulated that mbPDGF-BB transfer by D CD31EVs could account for VSMC resistance to apoptosis. By depleting CD31EVs of platelet-derived growth factor-BB (PDGF-BB) or blocking the PDGF receptor β on VSMCs, we demonstrated that mbPDGF-BB contributes to D CD31EV–mediated bak/bax and bcl-2 levels. Moreover, we found that bak expression is under the control of PDGF-BB–mediated microRNA (miR)-296-5p expression. In fact, while PDGF-BB treatment recapitulated D CD31EV–mediated antiapoptotic program and VSMC resistance to apoptosis, PDGF-BB–depleted CD31EVs failed. D CD31EVs also increased VSMC migration and recruitment to neovessels by means of PDGF-BB. Finally, we found that VSMCs, from human atherosclerotic arteries of individuals with T2D, express low bak/bax and high bcl-2 and miR-296-5p levels. This study identifies the mbPDGF-BB in D CD31EVs as a relevant mediator of diabetes-associated VSMC resistance to apoptosis.

Cardiovascular complications are a leading cause of morbidity and premature mortality in diabetes (1,2). Structural alterations to vessel walls result in intima-media thickening, which puts individuals at high risk of developing acute cardiovascular events (3,4). Moreover, restenosis is still a major complication in the diabetes setting. A main cause of reocclusion is intimal hyperplasia, which is due to the migration and/or excessive growth of vascular smooth muscle cells (VSMCs). A dysregulated balance between apoptosis and the proliferation of VSMCs seems to play a crucial role in intima-media thickening in individuals with diabetes (5,6). Indeed, in vitro studies have suggested that high glucose (HG) levels induce the expression of bcl-2 family members and inhibit the apoptotic protein inhibitor of apoptosis protein 1 (IAP-1) in VSMCs (7). In addition, Ruiz et al. (8) have demonstrated that VSMCs, recovered from patients with diabetes, show a resistance to apoptosis, which was possibly due to bcl-2 overexpression. Although circulating HG concentration might per se induce VSMC dysfunction, additional events can contribute to this process in vivo.

Several studies have focused on extracellular RNA transporters, indicating that they may be present in biological fluids in the form of vesicles, which have been denoted microvesicles, exosomes, membrane particles, and apoptotic bodies (9,10). Despite the lack of consensus on vesicle classification, the presence of overlapping characteristics and

[1]Department of Medical Sciences, University of Torino, Torino, Italy
[2]Department of Surgical, Medical, Molecular, and Critical Area Pathology, University of Pisa, Pisa, Italy

Corresponding authors: Maria Felice Brizzi, mariafelice.brizzi@unito.it, and Giovanni Camussi, giovanni.camussi@unito.it.

Received 24 March 2017 and accepted 22 January 2018.

This article contains Supplementary Data online at http://diabetes.diabetesjournals.org/lookup/suppl/doi:10.2337/db17-0371/-/DC1.

G.T. and P.D. contributed equally to this study.

biological activity has evoked the use of the inclusive term "extracellular vesicles" (EVs) (11,12). The paracrine/endocrine effects of EVs have recently gained significant attention (13,14). Indeed, EV biological activity has been linked to the transfer of bioactive molecules, including proteins and microRNA (miRs) (10–14). EVs are widely distributed in human body fluids, while circulating EV cargo usually reflects the cell of origin in its physiological and/or pathological condition (9–15). Indeed, the number and cargo of circulating EVs have been suggested as a means to predict the presence of disease and even the risk of developing disease (16,17).

Increased levels of circulating platelet- and endothelial cell (EC)-derived microparticles have been proposed as "biomarkers" of cell dysfunction (18,19). However, EVs might also deliver specific drivers of disease, as they behave as diffusible vectors of biological activity and participate in exchanging information. This study therefore investigates the role of EC-derived EVs as mediators of VSMC fate in type 2 diabetes (T2D).

RESEARCH DESIGN AND METHODS

Reagents and antibodies are reported in Supplementary Table 1.

Patients and Control Subjects

A total of 11 individuals with T2D and 6 individuals without diabetes (control subjects), who had undergone carotid endoarteriectomy surgery in our clinic, were included in the study. Clinical characteristics are reported in Supplementary Table 2. All individuals with diabetes were undergoing statin and metformin treatment. Ethics approval was obtained from Azienda Ospedaliero-Universitaria (AOU), Città della Salute e della Scienza di Torino, Torino, Italy. Informed consent was obtained from all individuals in accordance with the Declaration of Helsinki. We had no direct contact with the participants.

Isolation of VSMCs From Human Atherosclerotic Plaque Specimens

Human atherosclerotic plaque specimens were recovered from the above-reported subjects (T2D [D] and nondiabetic [ND] specimens) and processed as previously described (20). Vascular tissue was rinsed three times with PBS, and intima was removed in order to furnish the VSMCs. Tunica media were finely cut into 2- to 3-mm pieces and subjected to enzymatic digestion using collagenase type I (0.1 mg/mL) in DMEM for 1.5 h at 37°C. Digestion media were collected and filtered through nylon mesh cell strainers (100 μm) to remove the undigested explants. The resulting supernatants were centrifuged at 1,200 rpm for 10 min, and cells were plated at 2.5×10^4 cells/cm^2 and cultured with modified Eagle's medium supplemented with 20% (v/v) FBS and 1% penicillin-streptomycin. FACS analysis was performed on D VSMCs and ND VSMCs to characterize them, as previously described (20), using antibodies directed to CD31 and α-smooth muscle actin (α-SMA), directly or indirectly conjugated with fluorescein isothiocyanate (FITC) fluorochrome. FITC mouse nonimmune isotypic IgG (BD Bioscience Pharmingen) was used as control.

Cell Cultures

Primary macrovascular ECs and VSMCs were purchased from Lonza (Basel, Switzerland) and cultured as described by the manufacturer's instructions. VSMCs and ECs were used at II-III cell-culture passage. For collection of the EVs, ECs were starved under either low glucose (LG) (5 mmol/L) or HG (25 mmol/L) and for 24 h deprived of bovine calf serum. Cell viability was evaluated. Small interfering RNA (siRNA) technology was also used in HG-cultured ECs with siRNA negative control or the platelet-derived growth factor (PDGF)-BB siRNA (Applied Biosystems) (21). EV isolation was obtained from HG-cultured ECs depleted of PDGF-BB. In selected experiments, VSMCs were cultured in LG or HG and then treated in the presence of ND CD31EVs, D CD31EVs, or EC-derived EVs (5×10^3 EVs/target cell) or stimulated with PDGF-BB. In selected experiments, HG-cultured VSMCs were preincubated with a blocking PDGF receptor β (PDGFRβ) antibody (5 μg/mL). Details are reported in the Supplementary Data. All experiments were performed in accordance with European guidelines and policies and approved by the ethics committee of the University of Turin.

Isolation and Characterization of CD31EVs From Sera of Individuals With T2D and Individuals Without Diabetes

Human serum from all above-described individuals with T2D and control subjects was obtained before surgery and after informed consent. EVs from each participant were obtained by centrifuging serum as previously described (22). The supernatant was subsequently submitted to differential ultracentrifugation at 10,000*g* and 100,000*g* for 2 h at 4°C. EV pellets were then resuspended in DMEM and stored at −80°C. FACS analysis of D EVs and ND EVs was performed as previously described (23), using anti-CD31 allophycocyanin (APC), anti-CD14 phycoerythrin (PE), and anti-CD42b FITC antibodies. FITC, PE, or APC mouse nonimmune isotypic IgGs (BD Bioscience Pharmingen) were used as controls. FACS analysis was performed using a Guava easyCyte Flow Cytometer (Merck, Darmstadt, Germany). Fluorochrome-conjugated antibodies were added to a suspension of EVs (2.5×10^6 particles/100 μL) for 15 min at 4°C. Surface marker expression is reported in the representative histograms as the percentage of expression ± SD. The CD31 microbead kit (Miltenyi Biotec, Auburn, CA) was used to isolate CD31EVs from the sera of individuals with T2D (D CD31EVs) and control subjects (ND CD31EVs) (24). Briefly, 0.5 mL freshly thawed plasma was incubated with 100 μL CD31 microbeads for 4 h at 4°C. EVs captured on CD31 antibody–coated magnetic beads were recovered from the magnetic column (MS column) as described in the manufacturer's instructions. EV-bound beads were submitted to differential ultracentrifugation (Beckman Coulter Optima L-90K ultracentrifuge; Beckman Coulter, Fullerton, CA) for 3 h at 4°C. CD31EVs were either used fresh or were stored at −80°C and then processed for

transmission electron microscopy (TEM), biological effects, Western blot, and quantitative RT-PCR (qRT-PCR) analysis. CD63 content in CD31EVs was analyzed by Western blot. Details are reported in the Supplementary Data.

TEM

TEM was performed on CD31EVs that had been isolated by ultracentrifugation and resuspended in PBS, placed on 200 mesh nickel formvar carbon-coated grids (Electron Microscopy Science, Hatfield, PA), and left to adhere for 20 min. Grids were then processed as previously described (25) and observed under a Jeol JEM 1010 electron microscope (Jeol, Tokyo, Japan). Details are reported in the Supplementary Data.

Isolation of EC-Derived EVs

ECs were cultured in LG or HG DMEM without bovine calf serum for 24 h to collect the EVs from supernatants as previously described (21,22) and as detailed in the Supplementary Data. EV number and size distribution analysis was performed using a NanoSight LM10 (NanoSight Ltd, Minton Park, U.K.). Results were displayed as number per milliliters and as a frequency size distribution graph, output to a spreadsheet. EC-derived EVs (LG EVs or HG EVs) were processed for biological, Western blot and qRT-PCR analysis (21,22).

Western Blot Analysis

Cells and EVs were lysed and protein concentrations were obtained as previously described (25). Protein levels were normalized to α-SMA, β-actin, or CD63 content. Details are reported in the Supplementary Data.

EV Internalization

The internalization of EVs was evaluated using confocal microscopy (LSM5-PASCAL; Zeiss, Oberkochen, Germany) as previously described (25). EV pellets were added to HG-cultured VSMCs (2×10^4) pretreated or not with a blocking PDGFRβ antibody. Z-Stack confocal microscopy VSMC images were also obtained (25). Details are reported in the Supplementary Data.

RNA Isolation and Real-time qRT-PCR for miRs

Total RNA was isolated from the VSMCs of atherosclerotic plaque specimens and from human VSMCs, that had been treated as indicated or left untreated, using the TRIzol reagent (Invitrogen) as previously described (26). RNA from cells and EVs was then reverse transcribed using a TaqMan MicroRNA Reverse Transcription Kit, specific for miR-24-3p, miR-221, miR-222, and miR-296-5p, or a SYBR Green miRNA reverse transcription kit specific for miR-21-5p, miR-29a, and miR-145, as indicated. miR expression was normalized to the small nuclear RNA RNU6B. Loss- and gain-of-function experiments were performed in VSMCs that had been transfected with the anti-miR control, the anti–miR-296-5p, pre-miR control, or pre–miR-296-5p oligonucleotides (Applied Biosystems) according to the manufacturer's instructions (26). Details are reported in the Supplementary Data.

Luciferase miRNA Target Reporter Assay

The luciferase reporter assay was performed using a construct generated by subcloning the PCR products amplified from the full-length 3′ untranslated region (UTR) of human *BAK1* DNA into the Xba restriction site of the luciferase reporter vector pGL3 (Promega, Madison, WI). The PCR products were obtained using the primers for *BAK1* and are reported in detail in the Supplementary Data (26).

Cell Proliferation and Apoptosis Assay

Proliferative activity was assayed as previously described (27). For the apoptosis assay, VSMCs were subjected to Muse Annexin V and the cell dead assay (Merck, Darmstadt, Germany) in accordance with the manufacturer's instructions. Details are reported in the Supplementary Data.

Tubule-Like Structure Formation Assay

For analysis of the EC-VSMC interaction, 24-well plates were coated with growth factor–reduced Matrigel matrix (BD Biosciences) (28). Briefly, HG-cultured ECs and VSMCs were pretreated, for 24 h, with D CD31EVs, ND CD31EVs, or HG EVs that had been depleted, or not, of PDGF-BB. Red-labeled ECs (PKH26 vital dye) (4.5×10^4) were placed in HG medium on top of the polymerized matrix. Green-labeled VSMCs (PKH67 vital dye) (2×10^4) were then added to ECs. Details are reported in the Supplementary Data.

Scratch Assay on VSMCs

Scratch assays were performed on HG-cultured VSMCs, treated as indicated, to evaluate cell migration activity. VSMCs were seeded to a final density of 100,000 cells/well for 24 h in order to allow cell adhesion and the formation of a confluent monolayer to occur. Details are reported in the Supplementary Data.

ELISA Assays

PDGF-BB concentration in D CD31EVs was measured using a commercially available competitive enzyme immunoassay (ELISA) kit (R&D Systems, Minneapolis, MN) according to the manufacturer's instructions. For evaluation of mbPDGF-BB, intact or lysate D CD31EVs (2.5×10^8 particles) were compared. The same samples were pretreated with trypsin (0.25%) for 1 h (negative control). Details are reported in the Supplementary Data.

Statistical Analysis

All data are presented as mean ± SEM unless otherwise reported. The D'Agostino-Pearson test was used to test normality. Data on in vitro angiogenesis, cell proliferation, ELISA, apoptosis, and scratch assays; on qRT-PCR miR expression, loss- and gain-of-function experiments, and characterization of recovered EVs; and, lastly, on the densitometric analysis for Western blots were analyzed using the Student *t* tests for two-group comparison and using one-way ANOVA, followed by the Tukey multiple-comparison test, for three or more groups. All Western

blot experiments were performed in triplicate. The minimum sample size was four experiments performed in triplicate, thus ensuring 90% statistical power among experimental groups, and a probability level of 0.05 (two-tailed hypothesis). The cutoff for statistical significance was set at $P < 0.05$. All statistical analyses were carried out using GraphPad Prism, version 5.04 (GraphPad Software, Inc.).

RESULTS

D CD31EVs Potentiate VSMC Resistance to Apoptosis in HG Conditions

Circulating EVs are able to modulate cell fate (9,10,13). It was therefore decided to investigate whether and how circulating EVs, derived from ECs of individuals with T2D (D EVs), may impact on VSMC fate. Guava analysis was used to

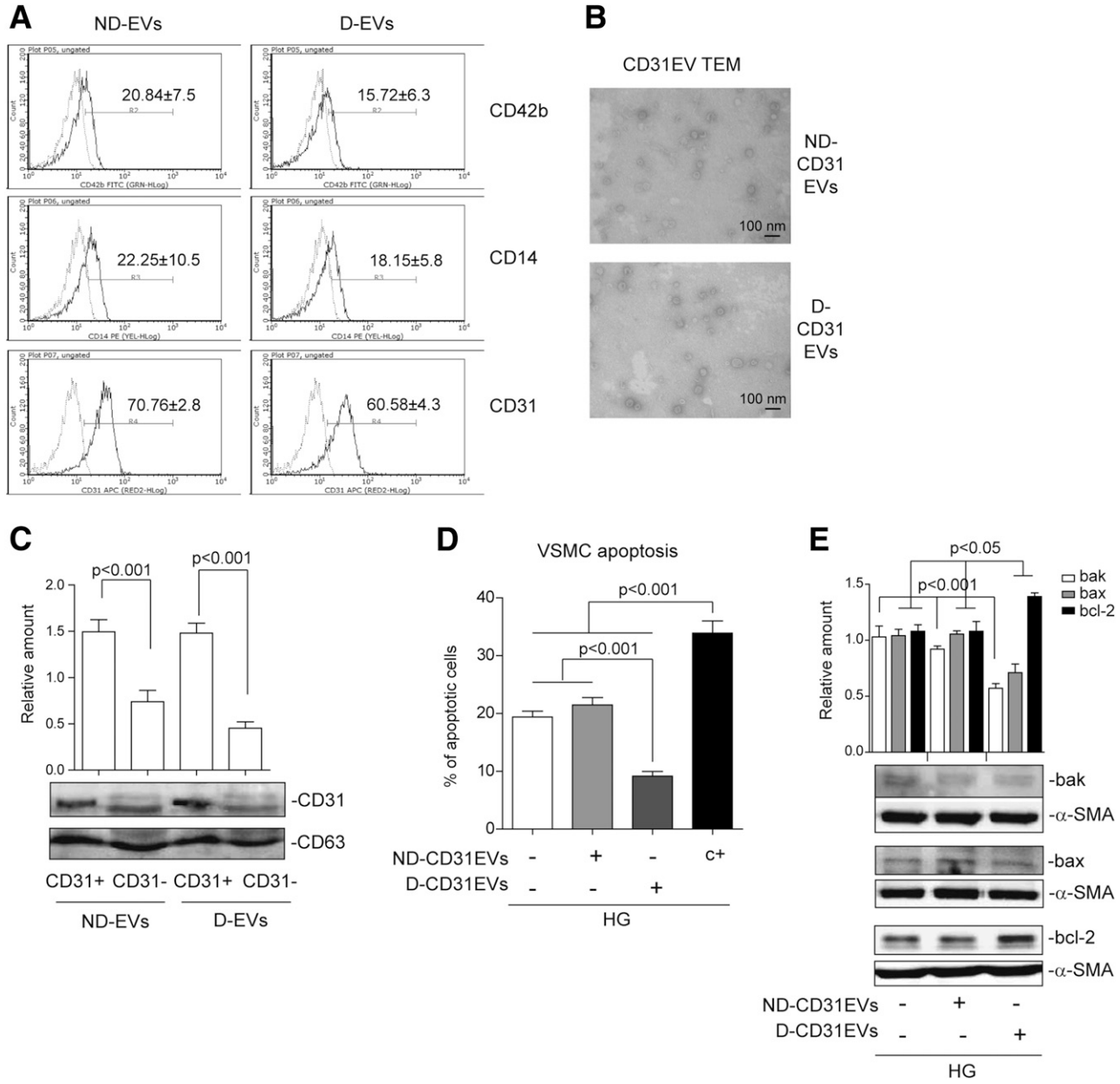

Figure 1—D CD31EVs increase VSMC survival. *A*: Representative FACS analysis of D ($n = 11$) and ND ($n = 6$) EVs; FITC CD42b, PE CD14, and APC CD31 were analyzed. All data are reported in the histograms (mean of percentage ± SD) ($P < 0.01$, D EVs vs. ND EVs for all markers). Isotype controls were included. GRN, green; RED2, red; YEL, yellow. *B*: Representative TEM imaging of D and ND CD31EVs negatively stained with NanoVan. JEOL Jem 1010 electron microscope was used. *C*: CD31EVs were lysed and evaluated for CD31 content ($CD31^+$), normalized to CD63. $CD31^-$ fraction was used as the negative control. The results are representative of all samples (D, $n = 11$; ND, $n = 6$) ($P < 0.001$, $CD31^+$ vs. $CD31^-$ fraction of individuals with T2D and individuals without diabetes). *D*: Apoptosis assay was applied to HG-cultured VSMCs, treated as indicated (mean percentage ± SEM of total apoptotic cells) ($n = 6$). Doxorubicin (1 μmol/L) was used as positive control (c+) ($P < 0.001$, all experimental conditions vs. positive control; $P < 0.001$, D CD31EVs vs. ND CD31EVs and none). *E*: Cell extracts from HG-cultured VSMCs, treated with D CD31EVs or ND CD31EVs, were analyzed for bak/bax and bcl-2 content, normalized to α-SMA ($P < 0.001$, D CD31EVs vs. ND CD31EVs and none for bak; $P < 0.05$, D CD31EVs vs. ND CD31EVs and none for bax and bcl-2) ($n = 6$).

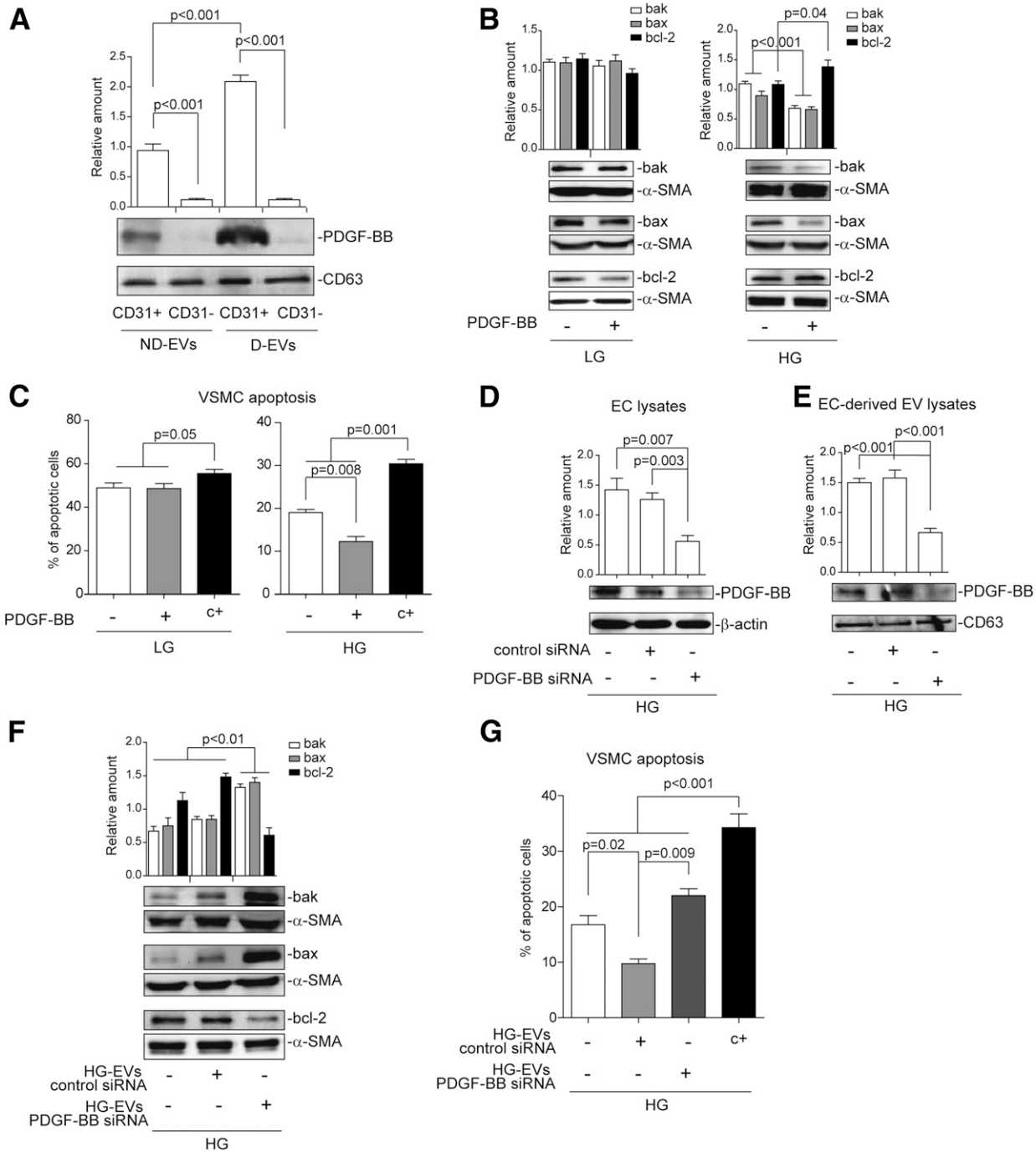

Figure 2—D CD31EVs enriched in PDGF-BB induce antiapoptotic signals. *A*: Negative and positive fractions of CD31EVs were analyzed by Western blot for PDGF-BB, normalized to CD63. The results are representative of all samples (D, $n = 11$; ND, $n = 6$) ($P < 0.001$, $CD31EV^+$ vs. $CD31EV^-$ of D and ND; $P < 0.001$, D $CD31EV^+$ vs. ND $CD31EV^+$ for PDGF-BB). *B*: Cell extracts from LG- and HG-cultured VSMCs untreated or treated with PDGF-BB (10 ng/mL) were analyzed for bak/bax and bcl-2 content, normalized to α-SMA (PDGF-BB vs. none in HG-cultured VSMCs, $P < 0.001$ for bak and bax and $P = 0.04$ for bcl-2) ($n = 5$). *C*: Apoptosis assay was applied to VSMCs, treated as in panel *B* (mean percentage ± SEM of total apoptotic cells) ($n = 6$). Doxorubicin (1 μmol/L) served as positive control (c+) (LG-cultured VSMCs, $P = 0.05$, all experimental conditions vs. positive control; HG-cultured VSMCs, $P = 0.001$, all experimental conditions vs. positive control, and $P = 0.008$, PDGF-BB vs. none). *D*: PDGF-BB content was evaluated in HG-cultured ECs transfected or not for 48 h with siRNA empty vector, used as control (control siRNA), or with PDGF-BB siRNA, and normalized to β-actin ($P = 0.007$, PDGF-BB siRNA vs. none, and $P = 0.003$, PDGF-BB siRNA vs. control siRNA). *E*: PDGF-BB content was evaluated in EVs recovered from HG-cultured ECs, treated as in panel *B*, and normalized to CD63 ($P < 0.001$, PDGF-BB siRNA vs. control siRNA and none). *F*: Cell extracts from HG-cultured VSMCs, treated as indicated, were analyzed for bak/bax and bcl-2 content, normalized to α-SMA ($P < 0.01$, HG EV PDGF-BB siRNA vs. HG EV control and none) ($n = 6$). *G*: Apoptosis assay was performed in HG-cultured VSMCs, treated as indicated (mean percentage ± SEM of total apoptotic cells) ($n = 6$). Doxorubicin (1 μmol/L) served as positive control ($P < 0.001$, all experimental conditions vs. positive control; $P = 0.02$, HG EV control siRNA vs. none; and $P = 0.009$, HG EV PDGF-BB siRNA vs. HG EV control siRNA).

demonstrate the presence of a high percentage of EVs of endothelial origin in the sera of control subjects (ND EVs) and of individuals with T2D (Fig. 1*A*). A significant reduction of D EVs was detected (Fig. 1*A*). EC-derived EVs from sera were therefore isolated using CD31-coated magnetic beads (ND CD31EVs and D CD31EVs) and analyzed using TEM (Fig. 1*B*) and Western blot (Fig. 1*C*). Functional studies were then performed to evaluate the biological relevance of D CD31EVs in mediating VSMC dysfunction in hyperglycemic condition (HG culture condition). LG-conditioned VSMCs served as control. Consistent with data provided by Ruiz et al. (8), we found that, unlike LG, HG treatment was associated with a significant upregulation of bcl-2 and downregulation of bak/bax (Supplementary Fig. 1*A*). By contrast, the expression of another member of the bcl-2 protein family, bcl2l2, did not change (Supplementary Fig. 1*B*). Moreover, HG treatment per se significantly decreased the number of apoptotic cells without affecting VSMC proliferation (Supplementary Fig. 1*C* and *D*). Functional studies were then performed on VSMCs cultured in HG conditions and treated with CD31EVs. As shown in Fig. 1*D*, D CD31EVs, unlike ND CD31EVs, further reduced both the number of apoptotic VSMCs and bak/bax content and increased bcl-2 level (Fig. 1*E*).

D CD31EVs Are Enriched in PDGF-BB

The transfer of proteins and/or genetic information into recipient cells is the main mechanism of EV action (9,10,13,14). CD31EV protein cargo and, in particular, the content of well-known VSMC proliferation/survival factor,

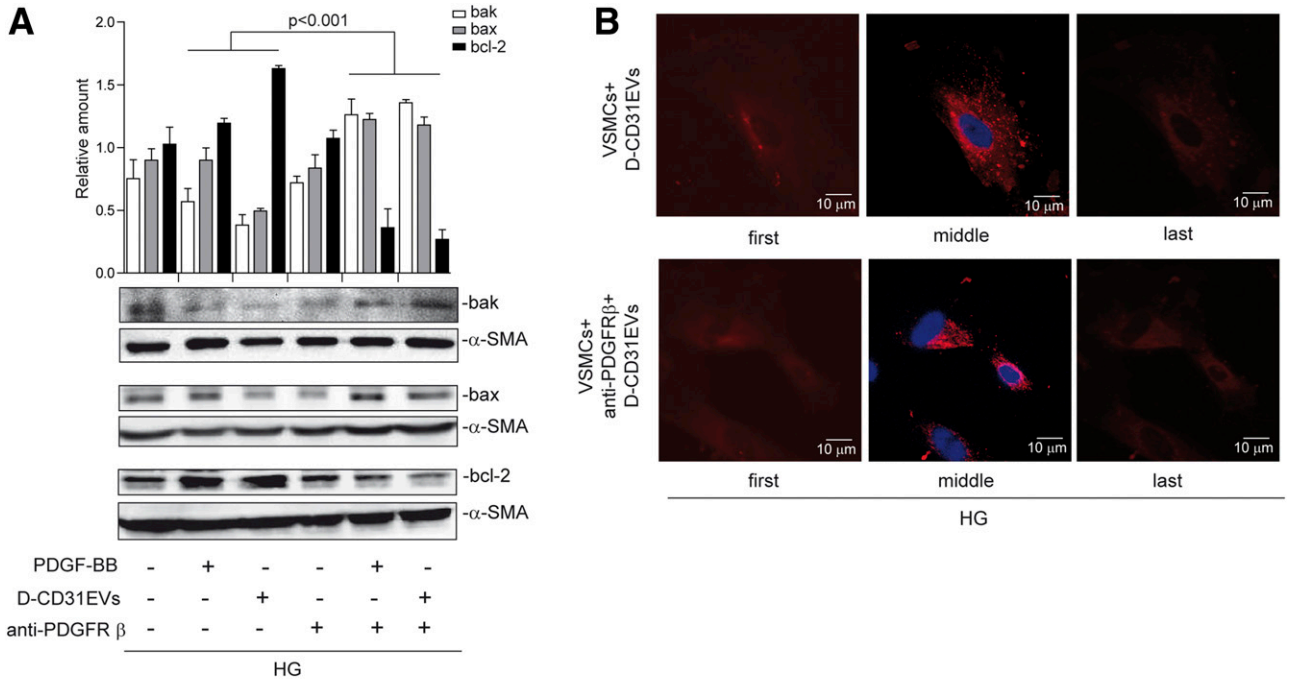

C

PDGF-BB (pg/ml)	
D-CD31EVs	25±4.7
D-CD31EV lysates	27±6.2
D-CD31EVs + trypsin	<15**

Figure 3—PDGFRβ blockade interferes with free PDGF-BB– and D CD31EV–mediated effects. *A*: HG-cultured VSMCs, preincubated or not with a blocking PDGFRβ antibody (5 μg/mL), were untreated or treated with PDGF-BB (10 ng/mL) or with D CD31EVs for 24 h. Cell extracts were analyzed for bak/bax and bcl-2 content, normalized to α-SMA ($P < 0.001$, PDGF-BB and D CD31EVs vs. PDGF-BB and D CD31EVs, pretreated with anti-PDGFRβ antibody) ($n = 4$). *B*: VSMC–D CD31EV uptake. VSMCs, preincubated or not with the blocking PDGFRβ antibody, were evaluated for the uptake of PKH26-labeled D CD31EVs and analyzed. DAPI was used as nuclear marker. Representative sections (first, middle, and last) of images (Z-Stack) obtained on a confocal microscope are reported. Four different experiments performed in triplicate ($n = 4$). Scale bars = 10 μm. *C*: For evaluation of mbPDGF-BB, intact or lysate D CD31EVs (2.5×10^8 particles), untreated or treated with trypsin (0.25%) for 1 h, were measured using a competitive enzyme immunoassay (ELISA) kit (**$P < 0.01$, intact and lysate D CD31EVs vs. D CD31EVs + trypsin) ($n = 3$).

PDGF-BB, were therefore analyzed in both CD31EVs and EVs recovered from LG- and HG-treated ECs. Supplementary Fig. 2*A* shows Nanosight analysis of EVs recovered from LG- or HG-cultured ECs (LG EVs or HG EVs). No differences in EV size or number between LG EVs and HG EVs were detected (data not shown). Conversely, PDGF-BB was found to be enriched only in D CD31EVs (Fig. 2*A*) and in HG EVs (Supplementary Fig. 2*B*).

Membrane-Bound PDGF-BB Drives D CD31EV Antiapoptotic Cues

LG- and HG-cultured VSMCs were treated with PDGF-BB to investigate the contribution of PDGF-BB in mediating D CD31EV biological effects. In fact, PDGF-BB further increased bcl-2 content, while reducing the number of apoptotic cells and bak/bax content, in HG-conditioned VSMCs. Conversely, these effects were not detected in VSMCs cultured in LG conditions (Fig. 2*B* and *C*). siRNA technology was therefore harnessed to abrogate PDGF-BB expression in EVs (Fig. 2*D* and *E*) and validate the role of PDGF-BB in regulating D CD31EV survival signals in HG conditions. As expected, PDGF-BB–depleted EVs no longer increased bcl-2 or decreased bak/bax expression (Fig. 2*F*) or the number of apoptotic cells (Fig. 2*G*). For investigation of whether different mechanisms might account for free PDGF-BB and D CD31EV–PDGF-BB–induced effects,

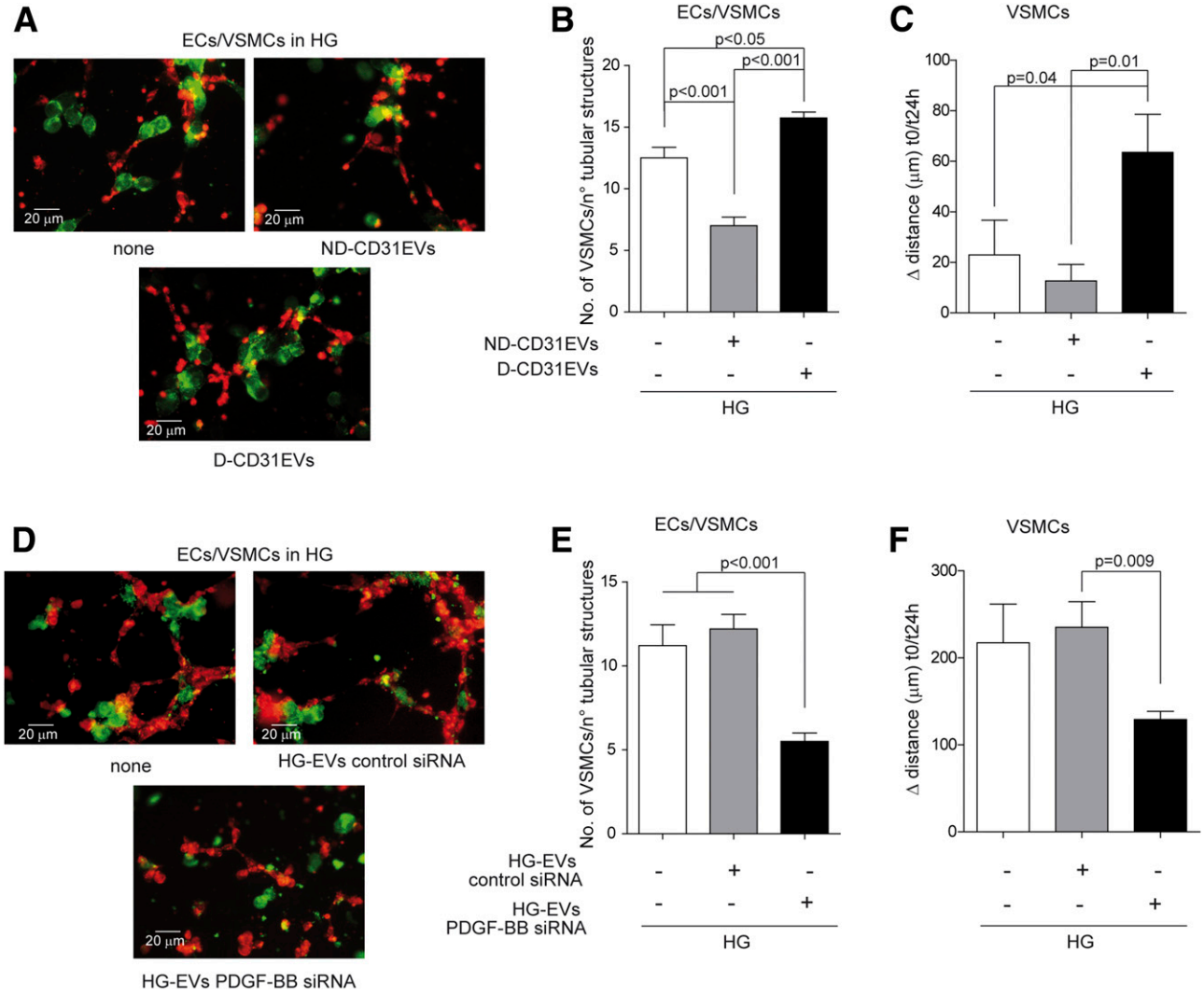

Figure 4—D CD31EVs increase VSMC migration and recruitment to tubule-like structures. *A* and *B*: An in vitro angiogenesis assay was performed using prelabeled ECs (red) and VSMCs (green) cocultured in HG medium with or without the indicated CD31EVs for 6 h (scale bars = 20 μm, ×40 magnification). Data are reported in the histogram as mean number ± SEM of VSMCs per number of tubular structures ($P <$ 0.001, ND CD31EVs vs. none and D CD31EVs; $P < 0.05$, D CD31EVs vs. none) ($n = 5$). *C*: VSMC migration assay was performed in HG conditions and with the indicated treatment ($n = 5$) (×20 magnification) ($P = 0.04$, D CD31EVs vs. none; $P = 0.01$, D CD31EVs vs. ND CD31EVs). *D* and *E*: An in vitro angiogenesis assay was performed, as in panel *A*, using HG EV control siRNA or HG EVs depleted of PDGF-BB (PDGF-BB siRNA) (scale bars = 20 μm, ×40 magnification). Data are reported in the histogram as mean number ± SEM of VSMCs per number of tubular structures ($P <$ 0.001, HG EV PDGF-BB siRNA vs. HG EV control siRNA and none) ($n = 5$). *F*: VSMC migration assay was performed in HG conditions under the indicated treatment ($n = 5$) (×20 magnification) ($P = 0.009$, HG EV PDGF-BB siRNA vs. HG EV control siRNA). Representative images were acquired on a confocal microscope.

HG-cultured VSMCs were pretreated with a blocking PDGFRβ antibody, stimulated with D CD31EVs or free PDGF-BB, and analyzed for bak/bax and bcl-2 expression. As shown in Fig. 3*A*, PDGFRβ blockade impacts on both free PDGF-BB and D CD31EV–mediated bak/bax and bcl-2 expression. To rule out the possibility that this effect depended on inhibition of PDGFRβ-mediated EV internalization, we performed Z-Stack analysis. Figure 3*B* shows that PDGFRβ blockade did not hamper EV internalization. Of note, the ELISA assay led to the discovery that PDGF-BB was anchored to the membrane of D CD31EVs (Fig. 3*C*), indicating that EV membrane-bound (mb)PDGF-BB, by binding to the PDGFRβ, might drive D CD31EV biological effects.

D CD31EVs Induce VSMC Migration and Recruitment to Neovessels via PDGF-BB–Mediated Effects

CD31EVs were also evaluated in an EC-VSMC coculture assay. A reduced number of vessels was detected in HG-cultured ECs (data not shown), and D CD31EVs nevertheless promoted VSMC recruitment to neo-formed tubule-like structures (Fig. 4*A* and *B*)—unlike ND CD31EVs. A scratch assay also highlighted increased VSMC motility upon D CD31EV treatment (Fig. 4*C*). As shown in Supplementary Fig. 2*C*, these effects did not depend on differences in EV vascular endothelial growth factor content. Furthermore, the contribution of PDGF-BB to both processes was validated in experiments using PDGF-BB–depleted EVs; such EVs failed to induce either effects (Fig. 4*D–F*).

D VSMCs Express High bcl-2 and Low bak/bax Content

For validation of the above results, VSMCs isolated from either D or ND human atherosclerotic plaque specimens were analyzed for bak/bax and bcl-2 expression. As shown in Fig. 5*A*, the majority of the recovered cells express VSMC marker. Moreover, as previously reported by Ruiz et al. (8), it was confirmed that D VSMCs expressed high bcl-2 levels. In addition, we found that D VSMCs also expressed low bak/bax content (Fig. 5*B* and *C*).

miR-296-5p Posttranscriptionally Controls bak Level in Response to HG and D CD31EVs

For further insight into the mechanisms regulating VSMC fate, the expression of miRs potentially involved in this process was first analyzed in D VSMCs and compared with ND VSMCs. As shown in Fig. 6*A*, no significant differences were detected in the expression of miR-21-5p, miR-24-3p, miR-145, miR-29a (not included in the panel: CT >38), miR-221, and miR-222 between D and ND VSMCs (29,30). Moreover, since bak, unlike bax, is one of miR-296-5p putative target genes (TarBase v7.0) (31), its expression was also analyzed. Indeed, high miR-296-5p levels were detected in D VSMCs (Fig. 6*A*). For validation of the role of miR-296-5p in controlling bak expression, VSMCs cultured in LG or HG conditions were analyzed for miR-296-5p expression. As shown in Fig. 6*B*, increased miR-296-5p expression was detected upon HG treatment. Moreover, the depletion of

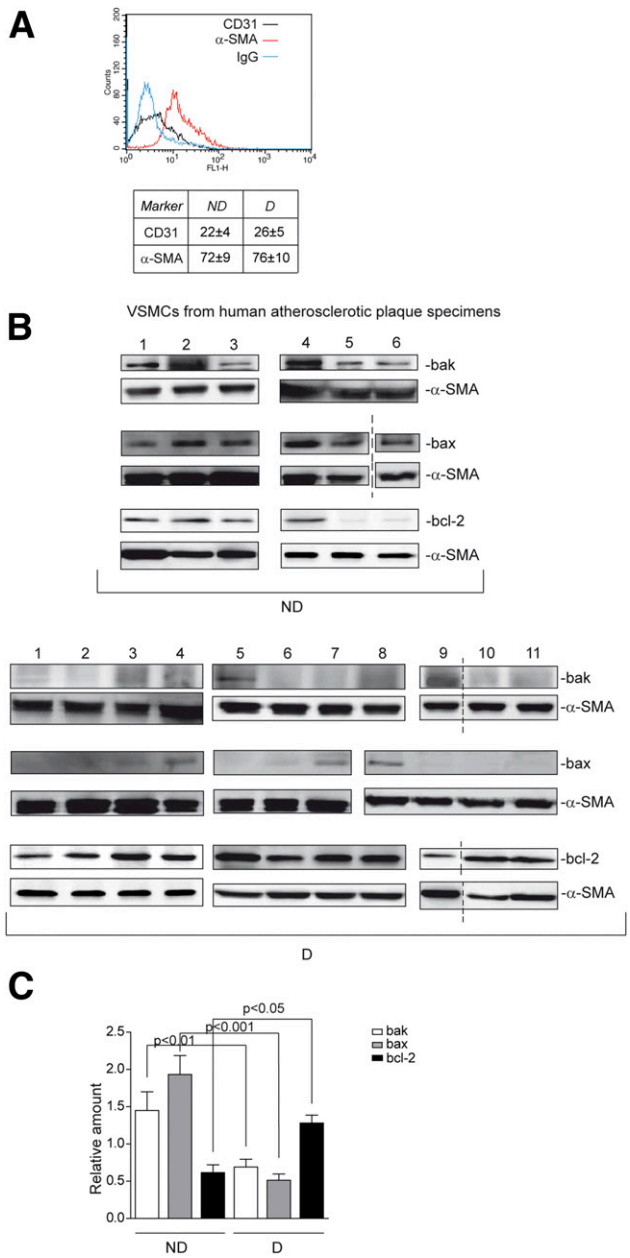

Figure 5—D VSMCs express high levels of bcl-2 and low bak/bax content. *A*: Representative FACS analysis of CD31 and α-SMA surface markers expressed by D (n = 11) and ND (n = 6) VSMCs. All data are reported in the table (mean percentage ± SD). Isotype control was included. FL1-H, fluorescence intensity. *B*: bak/bax and bcl-2 content were analyzed in all ND or D VSMC samples, normalized to α-SMA content. The statistical analysis of all samples (D, n = 11; ND, n = 6) is reported in *C* ($P < 0.01$, D vs. ND for bak; $P < 0.001$, D vs. ND for bax; and $P < 0.05$, D vs. ND for bcl-2).

miR-296-5p in HG-cultured VSMCs (Supplementary Fig. 3) led to the decrease of bcl-2 levels, the increase of bak/bax content (Fig. 6*C*), and a consistent increase in the number of apoptotic cells (Fig. 6*D*). For confirmation of the role of miR-296-5p in bak posttranscriptional regulation, the full-length 3′ UTR *BAK1* nucleotide sequence was analyzed for miR-296-5p blasting sequences revealing several base

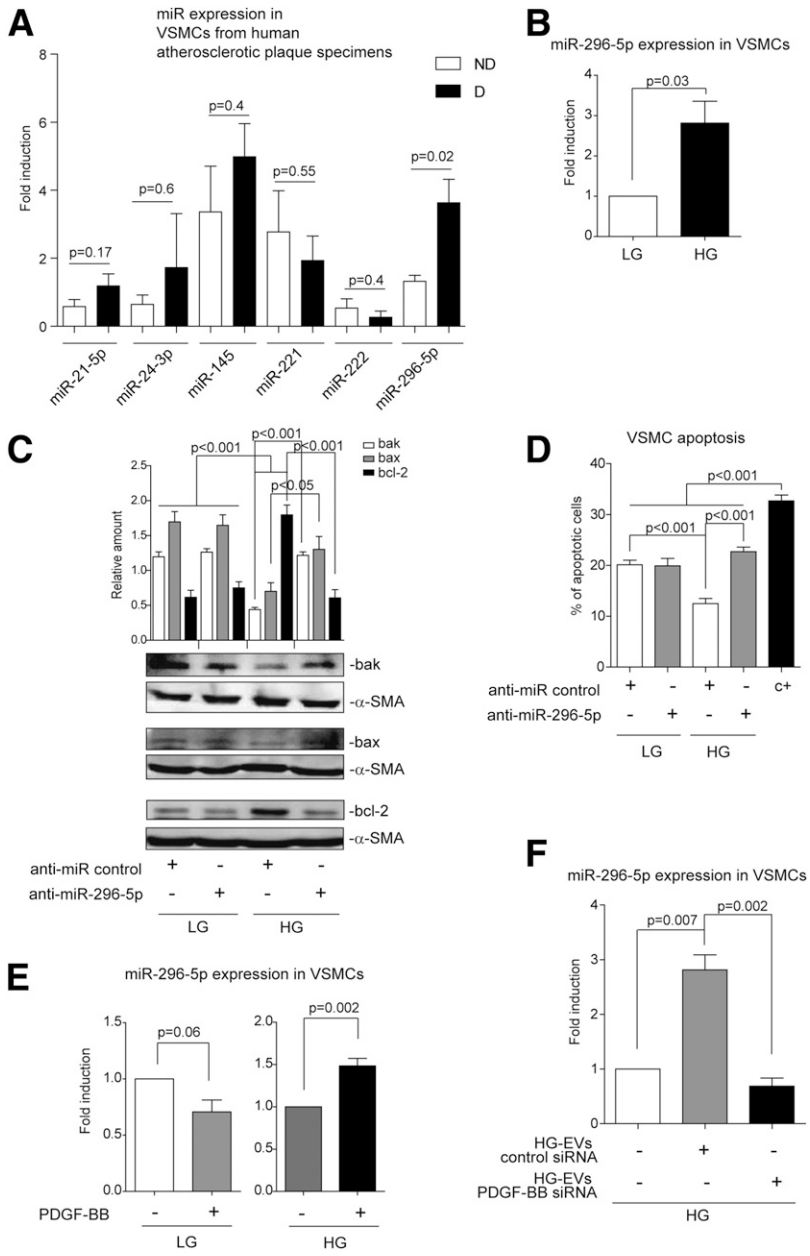

Figure 6—VSMC miR-296-5p expression is increased in hyperglycemic condition and boosted by PDGF-BB. *A*: The indicated miRs were evaluated by qRT-PCR in VSMCs recovered from D and ND human atherosclerotic plaque specimens. Data normalized to RNU6B are representative of all samples (D, $n = 11$; ND, $n = 6$) ($P = 0.02$, D vs. ND for miR-296-5p). *B*: miR-296-5p was evaluated by qRT-PCR on LG- or HG-treated VSMCs and normalized to RNU6B ($P = 0.03$, HG- vs. LG-treated VSMCs) ($n = 6$). *C*: Loss-of-function experiments were performed on LG- and HG-cultured VSMCs for 48 h, using anti-miR control or anti–miR-296-5p oligonucleotides. After 48 h, cells were lysed and analyzed for bak/bax and bcl-2 content, normalized to α-SMA ($P < 0.001$, LG anti-miR control and LG anti–miR-296-5p vs. HG anti-miR control for bak/bax and bcl-2; $P < 0.001$, HG anti-miR control vs. HG anti–miR-296-5p for bak and bcl-2; and $P < 0.05$, HG anti-miR control vs. HG anti–miR-296-5p for bax, $n = 3$). *D*: Apoptosis assay was performed on VSMCs cultured and treated as in *C*. Doxorubicin (1 μmol/L) served as positive control (c+). Data are expressed as mean percentage ± SEM ($n = 5$) of total apoptotic cells ($P < 0.001$, LG anti-miR control vs. HG anti-miR control and HG anti-miR control vs. HG anti–miR-296-5p; $P < 0.001$, all experimental conditions vs. positive control). *E*: miR-296-5p expression, normalized to RNU6B, was evaluated by qRT-PCR in LG- and HG-cultured VSMCs both with and without PDGF-BB (10 ng/mL) ($P = 0.002$, PDGF-BB vs. none in HG-treated VSMCs) ($n = 6$). *F*: miR-296-5p expression, normalized to RNU6B, was evaluated by qRT-PCR in HG-cultured VSMCs, treated as indicated ($P = 0.007$, HG EV siRNA empty vector, used as control [control siRNA] vs. none; $P = 0.002$, HG EV PDGF-BB siRNA vs. HG EV control siRNA) ($n = 6$).

pairings (1,138–1,158) (Fig. 7*A*). The luciferase assay was used to demonstrate that bak is indeed a direct miR-296-5p target (Fig. 7*B*). This observation was further validated by gain-of-function experiments (Fig. 7*C* and *D*).

For investigation of the contribution of PDGF-BB in mediating miR-296-5p expression, LG- and HG-cultured VSMCs were also treated with PDGF-BB. As shown in Fig. 6*E*, PDGF-BB further increased miR-296-5p only in

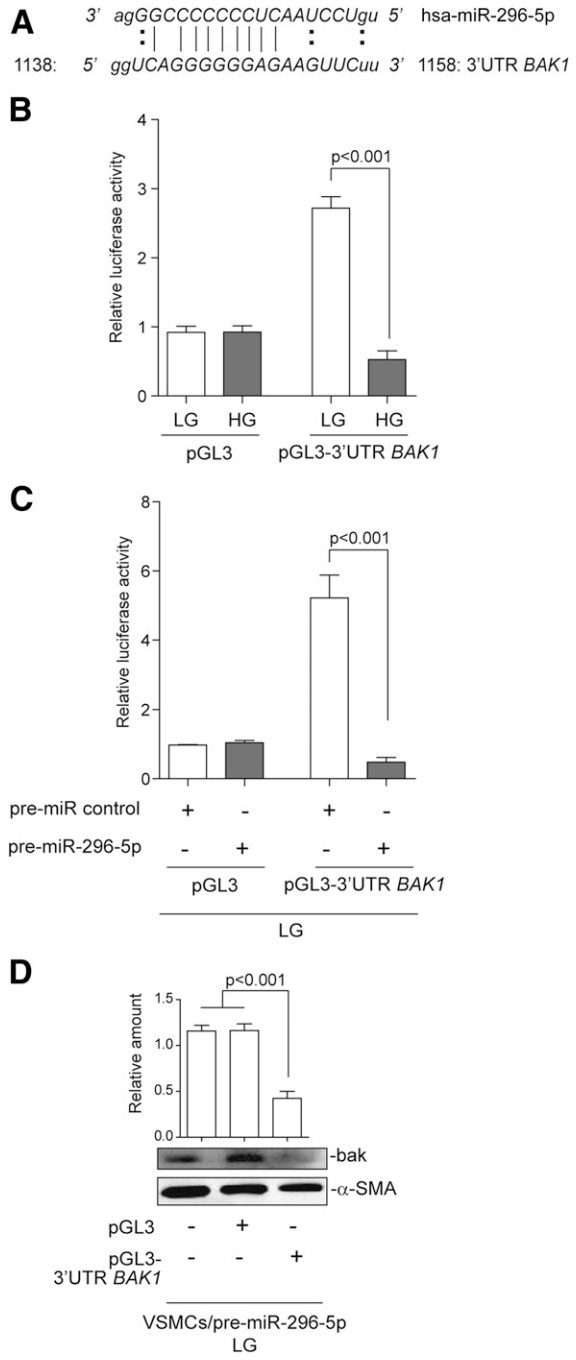

Figure 7—miR-296-5p posttranscriptionally regulates bak expression. *A*: Blast analysis of hsa-miR-296-5p sequence and *BAK1* 3′UTR full-length shows a base pairing from 1,138 to 1,158. *B*: pGL3 empty vector and pGL3–3′UTR *BAK1* luciferase constructs were transfected into LG- and HG-cultured VSMCs. Relative luciferase activity is reported ($P < 0.001$, HG vs. LG in pGL3–3′UTR *BAK1*-transfected cells, $n = 5$). *C*: pGL3 and pGL3–3′UTR *BAK1* constructs were transfected into LG-cultured VSMCs previously transfected with pre-miR control or with pre–miR-296-5p. Relative luciferase activity is reported ($P < 0.001$, pre–miR-296-5p vs. pre-miR control in pGL3–3′UTR *BAK1*–transfected cells) ($n = 5$). *D*: bak content was analyzed in cell extracts from VSMCs overexpressing miR-296-5p (pre–miR-296-5p), not transfected or transfected with pGL3 or pGL3–3′UTR *BAK1* constructs and normalized to α-SMA ($P < 0.001$, VSMCs/pre–miR-296-5p vs. none and pGL3 vs. pGL3-3′ UTR BAK1 in VSMCs/pre–miR-296-5p) ($n = 5$).

HG-cultured VSMCs. These results were validated by siRNA technology (Fig. 6*F*), thus suggesting that VSMC survival may be under the control of miR-296-5p.

D CD31EVs Are Almost Depleted of miR-296-5p Content

For exclusion of the possibility that D CD31EV–mediated effects could also depend on the delivery of miR-296-5p, the miR-296-5p content was also evaluated in CD31EVs and LG- or HG-cultured EC-derived EVs (LG EVs or HG EVs). Almost undetectable levels of miR-296-5p were found in D CD31EVs (Supplementary Fig. 2*D*) and in EVs from HG-treated ECs (Supplementary Fig. 2*E*). Thus, the role of mbPDGF-BB D CD31EVs in mediating miR-296-5p–driven posttranscriptional regulation of bak and its downstream events was further strengthened.

DISCUSSION

Atherosclerosis, and its associated complications, is a major cause of death worldwide (32). Diabetes accelerates atherosclerosis and restenosis after angioplasty (33,34). Indeed, increased VSMC migration and survival/proliferation are crucial for restenosis, particularly in those with diabetes (35–37). In vitro and ex vivo studies have shown that the upregulation of bcl-2/bcl-xl is crucial for VSMC resistance to apoptosis in diabetes (7,8,38,39). Moreover, Li et al. (7) have reported that while HG enhances the expression of bcl-2 family members in VSMCs, it reduced the expression of IAP-1. We herein demonstrate that VSMCs, exposed to HG concentrations, upregulate bcl-2 and downregulate bak/bax—without affecting VSMC proliferation. Moreover, we discovered that these effects are boosted by D CD31EV treatment. A cell's survival or death depends on the integrity of the mitochondrial outer membrane (40). In this regard, while the proapoptotic proteins, bak and bax, are involved in the permeabilization of mitochondrial outer membrane, the antiapoptotic bcl-2 family members counteract such proapoptotic signals by preventing cytochrome c efflux (40). Our results therefore indicate that an additional shift in the balance, from apoptotic to antiapoptotic signals, might be the main mechanism behind D CD31EV–induced resistance to apoptosis in HG conditions and suggest that hyperglycemia-mediated cues preferentially translate into VSMC resistance toward apoptosis rather than VSMC proliferation.

The genetic material in EV cargo has sparked considerable interest. The role of miRs as mediators of epigenetic changes has been extensively reported, particularly in diabetes (41,42). The transfer of miRs into recipient cells has been described as a relevant mechanism of EV biological action (9–14). As a matter of fact, Gu et al. (43) recently reported that the transfer of miR-195 from EC-derived EVs to VSMCs regulates VSMC proliferation. Despite the ability of D CD31EVs to induce functional changes in VSMCs, our results demonstrate that D CD31EV–mediated VSMC dysfunction relies on a mechanism independent of the delivery of miRs. Indeed, EVs also transport and deliver proteins that can affect VSMC fate, including PDGF-BB. PDGF-BB

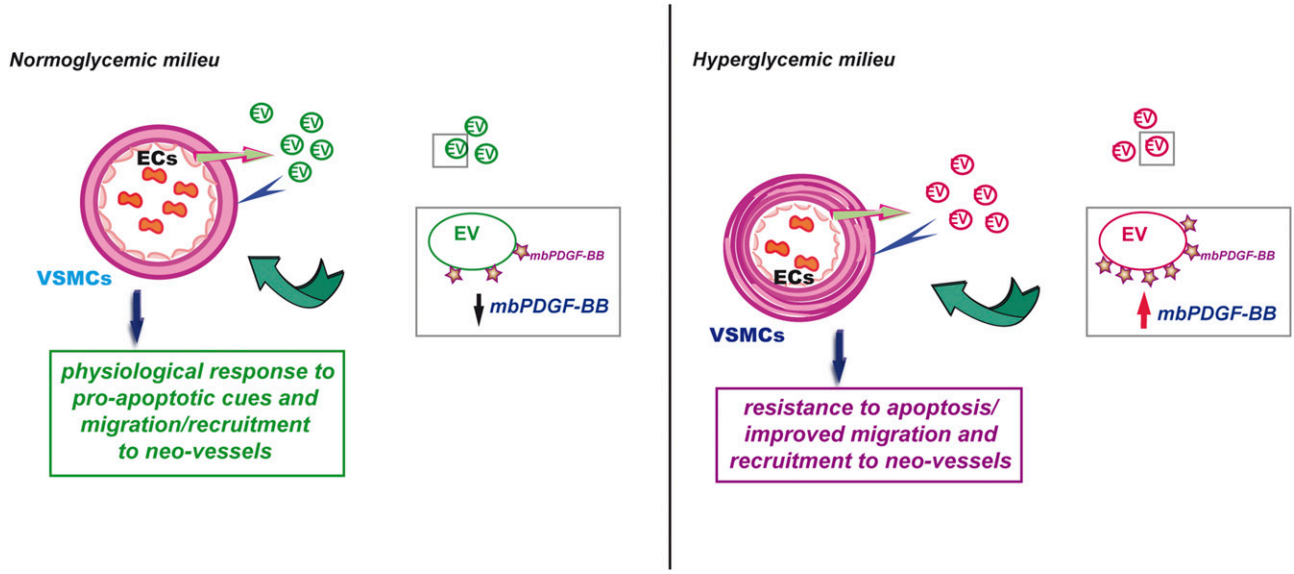

Figure 8—Schematic representation of HG and D CD31EV mechanism of action. ND CD31EVs do not affect VSMC fate owing to their low mbPDGF-BB content (left panel). In the diabetes setting, D CD31EVs enriched in mbPDGF-BB content affect VSMC fate by promoting resistance to apoptosis (right panel).

is a growth factor known to regulate VSMC outcomes (44,45). In this regard, PDGF-BB derived from platelet and EC is considered a relevant mediator of VSMC dysfunction and restenosis (46). As a matter of fact, we demonstrate that D CD31EVs are enriched in PDGF-BB and that PDGF-BB–enriched D CD31EVs contribute to VSMC dysfunction in the setting of diabetes. Several lines of evidence indicate that downstream signaling events, activated by PDGF-BB, trigger various biological processes, including VSMC migration and recruitment to neo-formed vessels (44,45). It is worth noting that PDGF-BB–depleted EVs failed to induce both VSMC migration and recruitment to neovessels. This suggests that CD31EV–PDGF-BB cargo might play a crucial role in accelerating VSMC dysfunction and restenosis in T2D.

PDGF-BB synthesis and release can increase in response to various stimuli including intima damage (47). As shown herein, in the diabetes setting, CD31EVs constitute a relevant circulating PDGF-BB reservoir and contribute to VSMC fate. We established that PDGF-BB is bound to the membrane of CD31EVs and is required for their biological action but not for their internalization. As a proof of concept, PDGFRβ blockade completely hampers CD31EV-mediated bak/bax expression without impeding their entry into the cell. This indicates that, along with free PDGF-BB, mbPDGF-BB–enriched D CD31EVs contribute to PDGF-BB paracrine effects (48). A cooperative action between CD31EVs and platelet-derived EVs could be postulated in vivo. In fact, EVs released from platelets accumulate in human atherosclerotic plaques and can induce major biological pathways by transferring their PDGF-BB content (49). In line with the results presented herein, it has recently been reported that EC- and platelet-derived EVs are enriched in PDGF-BB in patients with cardiovascular diseases (50).

miRs are key regulators of gene expression, mainly at the posttranscriptional level (51). We herein demonstrate, both ex vivo and in vitro, that the hyperglycemia milieu enhances miR-296-5p expression and modulates bak content in VSMCs and that these effects are strictly dependent on D CD31EV–PDGF-BB cargo rather than EV miR-296-5p delivery. In addition, a shift between antiapoptotic to proapoptotic signals after PDGFRβ blockade (downregulation of bcl-2 expression) was observed. This suggests that PDGF-BB directly, or indirectly by changing the balance of cellular miRs, might transcriptionally or posttranscriptionally regulate its expression. Mutually, these events translate in VSMC resistance to apoptosis.

Emerging evidence suggests that EVs can serve as specific diagnostic/prognostic biomarkers, since they can provide intercellular state information on a given disease condition (52). Increased levels of "small (submicroscopic) membranous particles" of endothelial origin, such as $CD31^{+}$/annexin V^{+} and $CD31^{+}/CD42^{-}$, have been detected in circulation in patients with coronary artery disease, suggesting that they may be an additional risk stratification factor (18,19). A significant reduction in CD31EVs ($CD31^{high}/CD42b^{low}/CD14^{low}$) has been found in individuals with T2D in the current study. The phenotype of the "small membrane particles," which also includes apoptotic bodies, and the lack of exosome refining (18,19) in coronary artery disease patient studies could explain the discrepancy with our results. However, increasing amounts of evidence indicate that healthy subjects and diseased individuals release EVs with different cargo into circulation (53). Our ex vivo and in vitro results reinforce the notion that D CD31EV

cargo, rather than D CD31EV number, is the crucial determinant of their biological activity.

The current study reports that hyperglycemia per se induces epigenetic mechanisms in VSMCs by enriching the circulating CD31EV cargo with mbPDGF-BB, which translates into VSMC resistance to apoptosis (Fig. 8). We are also the first to demonstrate that EV–mbPDGF-BB–mediated miR-296-5p overexpression, and the posttranscriptional regulation of bak, is a relevant mechanism of D CD31EV action. Overall, these results identify D CD31EV–mbPDGF-BB as a novel driver of VSMC dysfunction in the setting of diabetes.

Funding. This work was supported by grants from Ministero dell'Università e della Ricerca Scientifica (ex 60%) (to P.D.) and was also supported by Associazione Italiana per la Ricerca sul Cancro project IG 2015.17630 (to M.F.B.).

Duality of Interest. This work was also supported grant no. 071215 from Unicyte to G.C. and M.F.B. No other potential conflicts of interest relevant to this article were reported.

Author Contributions. G.T. performed ex vivo and in vitro experiments and miR and protein analysis. P.D. performed in vitro angiogenesis assay and FACS analysis. A.R. generated constructs and performed transfections. G.L. performed in vitro experiments and EV isolation. M.G. performed loss- and gain-of-function experiments. S.G. performed Western blot analysis. C.G. performed EV isolation and characterization. A.S. contributed to data interpretation and revised the manuscript. G.C. contributed to the study conception and revised the manuscript. M.F.B. contributed to the study conception, designed the study, and wrote the manuscript. M.F.B. is the guarantor of this work and, as such, had full access to all the data in the study and takes responsibility for the integrity of the data and the accuracy of the data analysis.

References

1. Sarwar N, Gao P, Seshasai SR, et al.; Emerging Risk Factors Collaboration. Diabetes mellitus, fasting blood glucose concentration, and risk of vascular disease: a collaborative meta-analysis of 102 prospective studies [published correction appears in Lancet 2010;376:958]. Lancet 2010;375:2215–2222

2. Fox CS, Golden SH, Anderson C, et al.; American Heart Association Diabetes Committee of the Council on Lifestyle and Cardiometabolic Health; Council on Clinical Cardiology, Council on Cardiovascular and Stroke Nursing, Council on Cardiovascular Surgery and Anesthesia, Council on Quality of Care and Outcomes Research; American Diabetes Association. Update on prevention of cardiovascular disease in adults with type 2 diabetes mellitus in light of recent evidence: a scientific statement from the American Heart Association and the American Diabetes Association. Circulation 2015;132:691–718

3. Terry JG, Tang R, Espeland MA, et al. Carotid arterial structure in patients with documented coronary artery disease and disease-free control subjects. Circulation 2003;107:1146–1151

4. Schram MT, Henry RM, van Dijk RA, et al. Increased central artery stiffness in impaired glucose metabolism and type 2 diabetes: the Hoorn Study. Hypertension 2004;43:176–181

5. Gomez D, Owens GK. Smooth muscle cell phenotypic switching in atherosclerosis. Cardiovasc Res 2012;95:156–164

6. Goel SA, Guo LW, Liu B, Kent KC. Mechanisms of post-intervention arterial remodelling. Cardiovasc Res 2012;96:363–371

7. Li H, Télémaque S, Miller RE, Marsh JD. High glucose inhibits apoptosis induced by serum deprivation in vascular smooth muscle cells via upregulation of Bcl-2 and Bcl-xl. Diabetes 2005;54:540–545

8. Ruiz E, Gordillo-Moscoso A, Padilla E, et al. Human vascular smooth muscle cells from diabetic patients are resistant to induced apoptosis due to high Bcl-2 expression. Diabetes 2006;55:1243–1251

9. Simons M, Raposo G. Exosomes–vesicular carriers for intercellular communication. Curr Opin Cell Biol 2009;21:575–581

10. Mause SF, Weber C. Microparticles: protagonists of a novel communication network for intercellular information exchange. Circ Res 2010;107:1047–1057

11. Théry C, Ostrowski M, Segura E. Membrane vesicles as conveyors of immune responses. Nat Rev Immunol 2009;9:581–593

12. Gould SJ, Raposo G. As we wait: coping with an imperfect nomenclature for extracellular vesicles. J Extracell Vesicles 2013;2:20389

13. Camussi G, Deregibus MC, Bruno S, Cantaluppi V, Biancone L. Exosomes/microvesicles as a mechanism of cell-to-cell communication. Kidney Int 2010;78:838–848

14. Ratajczak MZ, Ratajczak J. Horizontal transfer of RNA and proteins between cells by extracellular microvesicles: 14 years later. Clin Transl Med 2016;5:7

15. Yuana Y, Sturk A, Nieuwland R. Extracellular vesicles in physiological and pathological conditions. Blood Rev 2013;27:31–39

16. Chironi G, Simon A, Hugel B, et al. Circulating leukocyte-derived microparticles predict subclinical atherosclerosis burden in asymptomatic subjects. Arterioscler Thromb Vasc Biol 2006;26:2775–2780

17. Ueba T, Nomura S, Inami N, et al. Plasma level of platelet-derived microparticles is associated with coronary heart disease risk score in healthy men. J Atheroscler Thromb 2010;17:342–349

18. Sinning JM, Losch J, Walenta K, Böhm M, Nickenig G, Werner N. Circulating CD31+/Annexin V+ microparticles correlate with cardiovascular outcomes. Eur Heart J 2011;32:2034–2041

19. Jung KH, Chu K, Lee ST, et al. Risk of macrovascular complications in type 2 diabetes mellitus: endothelial microparticle profiles. Cerebrovasc Dis 2011;31:485–493

20. Brizzi MF, Formato L, Dentelli P, et al. Interleukin-3 stimulates migration and proliferation of vascular smooth muscle cells: a potential role in atherogenesis. Circulation 2001;103:549–554

21. Togliatto G, Dentelli P, Gili M, et al. Obesity reduces the pro-angiogenic potential of adipose tissue stem cell-derived extracellular vesicles (EVs) by impairing miR-126 content: impact on clinical applications. Int J Obes 2016;40:102–111

22. Deregibus MC, Cantaluppi V, Calogero R, et al. Endothelial progenitor cell derived microvesicles activate an angiogenic program in endothelial cells by a horizontal transfer of mRNA. Blood 2007;110:2440–2448

23. Bruno S, Grange C, Collino F, et al. Microvesicles derived from mesenchymal stem cells enhance survival in a lethal model of acute kidney injury. PLoS One 2012;7:e33115

24. Greening DW, Xu R, Ji H, Tauro BJ, Simpson RJ. A protocol for exosome isolation and characterization: evaluation of ultracentrifugation, density-gradient separation, and immunoaffinity capture methods. Methods Mol Biol 2015;1295:179–209

25. Lombardo G, Dentelli P, Togliatto G, et al. Activated stat5 trafficking via endothelial cell-derived extracellular vesicles controls IL-3 pro-angiogenic paracrine action. Sci Rep 2016;6:25689

26. Gallo S, Gili M, Lombardo G, et al. Stem cell-derived, microRNA-carrying extracellular vesicles: a novel approach to interfering with mesangial cell collagen production in a hyperglycaemic setting. PLoS One 2016;11:e0162417

27. Dentelli P, Barale C, Togliatto G, et al. A diabetic milieu promotes OCT4 and NANOG production in human visceral-derived adipose stem cells. Diabetologia 2013;56:173–184

28. Zeoli A, Dentelli P, Rosso A, et al. Interleukin-3 promotes expansion of hemopoietic-derived CD45+ angiogenic cells and their arterial commitment via STAT5 activation. Blood 2008;112:350–361

29. Shantikumar S, Caporali A, Emanueli C. Role of microRNAs in diabetes and its cardiovascular complications. Cardiovasc Res 2012;93:583–593

30. Wei Y, Schober A, Weber C. Pathogenic arterial remodeling: the good and bad of microRNAs. Am J Physiol Heart Circ Physiol 2013;304:H1050–H1059

31. Karginov FV, Hannon GJ. Remodeling of Ago2-mRNA interactions upon cellular stress reflects miRNA complementarity and correlates with altered translation rates. Genes Dev 2013;27:1624–1632

32. GBD 2013 Mortality and Causes of Death Collaborators. Global, regional, and national age-sex specific all-cause and cause-specific mortality for 240 causes of death, 1990-2013: a systematic analysis for the Global Burden of Disease Study 2013. Lancet 2015;385:117–171
33. Kornowski R, Mintz GS, Kent KM, et al. Increased restenosis in diabetes mellitus after coronary interventions is due to exaggerated intimal hyperplasia. A serial intravascular ultrasound study. Circulation 1997;95:1366–1369
34. Brooks MM, Jones RH, Bach RG, et al.; BARI Investigators. Predictors of mortality and mortality from cardiac causes in the Bypass Angioplasty Revascularization Investigation (BARI) randomized trial and registry. Circulation 2000;101:2682–2689
35. Henry RM, Kostense PJ, Dekker JM, et al. Carotid arterial remodeling: a maladaptive phenomenon in type 2 diabetes but not in impaired glucose metabolism: the Hoorn study. Stroke 2004;35:671–676
36. Watson PA, Nesterova A, Burant CF, Klemm DJ, Reusch JE. Diabetes-related changes in cAMP response element-binding protein content enhance smooth muscle cell proliferation and migration. J Biol Chem 2001;276:46142–46150
37. Yasunari K, Kohno M, Kano H, Yokokawa K, Minami M, Yoshikawa J. Antioxidants improve impaired insulin-mediated glucose uptake and prevent migration and proliferation of cultured rabbit coronary smooth muscle cells induced by high glucose. Circulation 1999;99:1370–1378
38. Hall JL, Matter CM, Wang X, Gibbons GH. Hyperglycemia inhibits vascular smooth muscle cell apoptosis through a protein kinase C-dependent pathway. Circ Res 2000;87:574–580
39. Sakuma H, Yamamoto M, Okumura M, Kojima T, Maruyama T, Yasuda K. High glucose inhibits apoptosis in human coronary artery smooth muscle cells by increasing bcl-xL and bfl-1/A1. Am J Physiol Cell Physiol 2002;283:C422–C428
40. Karch J, Molkentin JD. Regulated necrotic cell death: the passive aggressive side of Bax and Bak. Circ Res 2015;116:1800–1809
41. Guay C, Regazzi R. Circulating microRNAs as novel biomarkers for diabetes mellitus. Nat Rev Endocrinol 2013;9:513–521
42. Togliatto G, Dentelli P, Brizzi MF. Skewed epigenetics: an alternative therapeutic option for diabetes complications. J Diabetes Res 2015;2015:373708
43. Gu J, Zhang H, Ji B, et al. Vesicle miR-195 derived from endothelial cells inhibits expression of serotonin transporter in vessel smooth muscle cells. Sci Rep 2017;7:43546
44. Grotendorst GR, Chang T, Seppä HEJ, Kleinman HK, Martin GR. Platelet-derived growth factor is a chemoattractant for vascular smooth muscle cells. J Cell Physiol 1982;113:261–266
45. Bilato C, Pauly RR, Melillo G, et al. Intracellular signaling pathways required for rat vascular smooth muscle cell migration. Interactions between basic fibroblast growth factor and platelet-derived growth factor. J Clin Invest 1995;96:1905–1915
46. McNamara CA, Sarembock IJ, Bachhuber BG, et al. Thrombin and vascular smooth muscle cell proliferation: implications for atherosclerosis and restenosis. Semin Thromb Hemost 1996;22:139–144
47. Andrae J, Gallini R, Betsholtz C. Role of platelet-derived growth factors in physiology and medicine. Genes Dev 2008;22:1276–1312
48. Raines EW. PDGF and cardiovascular disease. Cytokine Growth Factor Rev 2004;15:237–254
49. Weber A, Köppen HO, Schrör K. Platelet-derived microparticles stimulate coronary artery smooth muscle cell mitogenesis by a PDGF-independent mechanism. Thromb Res 2000;98:461–466
50. Goetzl EJ, Schwartz JB, Mustapic M, et al. Altered cargo proteins of human plasma endothelial cell-derived exosomes in atherosclerotic cerebrovascular disease. FASEB J 2017;31:3689–3694
51. Tüfekci KU, Meuwissen RL, Genç S. The role of microRNAs in biological processes. Methods Mol Biol 2014;1107:15–31
52. Barile L, Vassalli G. Exosomes: therapy delivery tools and biomarkers of diseases. Pharmacol Ther 2017;174:63–78
53. Pant S, Hilton H, Burczynski ME. The multifaceted exosome: biogenesis, role in normal and aberrant cellular function, and frontiers for pharmacological and biomarker opportunities. Biochem Pharmacol 2012;83:1484–1494